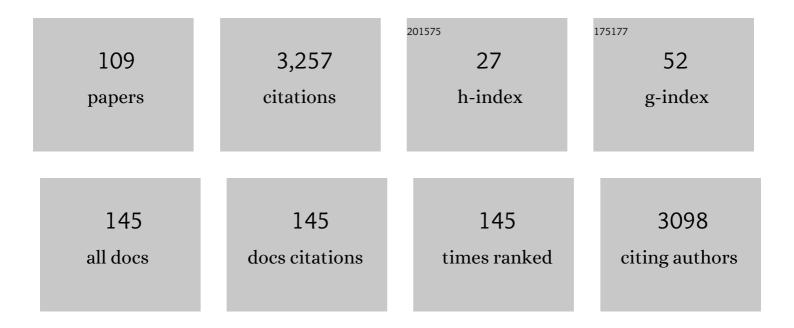
List of Publications by Year in descending order

Source: https://exaly.com/author-pdf/48842/publications.pdf Version: 2024-02-01



EDCAR C RUCK

#	Article	IF	CITATIONS
1	Ten-year results from unsaturated drip tests with UO2 at 90°C: implications for the corrosion of spent nuclear fuel. Journal of Nuclear Materials, 1996, 238, 78-95.	1.3	258
2	Synthesis, Characterization, and Manipulation of Helical SiO2 Nanosprings. Nano Letters, 2003, 3, 577-580.	4.5	198
3	Imaging Hydrated Microbial Extracellular Polymers: Comparative Analysis by Electron Microscopy. Applied and Environmental Microbiology, 2011, 77, 1254-1262.	1.4	168
4	Contaminant Uranium Phases and Leaching at the Fernald Site in Ohio. Environmental Science & Technology, 1996, 30, 81-88.	4.6	157
5	Review of the Scientific Understanding of Radioactive Waste at the U.S. DOE Hanford Site. Environmental Science & Technology, 2018, 52, 381-396.	4.6	130
6	Towards data-driven next-generation transmission electron microscopy. Nature Materials, 2021, 20, 274-279.	13.3	130
7	Immobilization of 99-Technetium (VII) by Fe(II)-Goethite and Limited Reoxidation. Environmental Science & Technology, 2011, 45, 4904-4913.	4.6	124
8	Influence of Dynamical Conditions on the Reduction of U ^{VI} at the Magnetiteâ^'Solution Interface. Environmental Science & Technology, 2010, 44, 170-176.	4.6	110
9	Oxidative Corrosion of Spent uo ₂ Fuel in Vapor and Dripping Groundwater at 90°C. Materials Research Society Symposia Proceedings, 1999, 556, 431.	0.1	98
10	Corrosion of commercial spent nuclear fuel. 1. Formation of studtite and metastudtite. Radiochimica Acta, 2005, 93, .	0.5	89
11	Radiation damage effects in candidate titanates for Pu disposition: Pyrochlore. Journal of Nuclear Materials, 2005, 345, 109-135.	1.3	86
12	Determination of the uranium valence state in the brannerite structure using EELS, XPS, and EDX. Physics and Chemistry of Minerals, 2005, 32, 52-64.	0.3	83
13	A new uranyl oxide hydrate phase derived from spent fuel alteration. Journal of Nuclear Materials, 1997, 249, 70-76.	1.3	73
14	Uranium. , 2008, , 253-698.		71
15	The chemistry of the light rareâ€earth elements as determined by electron energy loss spectroscopy. Applied Physics Letters, 1996, 68, 3817-3819.	1.5	69
16	EELS analysis of redox in glasses for plutonium immobilization. Ultramicroscopy, 1997, 67, 77-81.	0.8	63
17	Microanalysis of colloids and suspended particles from nuclear waste glass alteration. Applied Geochemistry, 1999, 14, 635-653.	1.4	53
18	Radiation damage effects in candidate titanates for Pu disposition: Zirconolite. Journal of Nuclear Materials, 2008, 372, 16-31.	1.3	52

#	Article	IF	CITATIONS
19	Neptunium(V) Partitioning to Uranium(VI) Oxide and Peroxide Solids. Environmental Science & Technology, 2005, 39, 4117-4124.	4.6	49
20	On the mechanical stability of uranyl peroxide hydrates: implications for nuclear fuel degradation. RSC Advances, 2015, 5, 79090-79097.	1.7	46
21	Lithium-Assisted Self-Assembly of Aluminum Carbide Nanowires and Nanoribbons. Nano Letters, 2002, 2, 105-108.	4.5	45
22	Corrosion of commercial spent nuclear fuel. 2. Radiochemical analyses of metastudtite and leachates. Radiochimica Acta, 2005, 93, 169-175.	0.5	45
23	Importance of interlayer H bonding structure to the stability of layered minerals. Scientific Reports, 2017, 7, 13274.	1.6	42
24	Heterogeneous Reduction of PuO ₂ with Fe(II): Importance of the Fe(III) Reaction Product. Environmental Science & Technology, 2011, 45, 3952-3958.	4.6	38
25	Microscale characterization of uranium(VI) silicate solids and associated neptunium(V). Radiochimica Acta, 2005, 93, .	0.5	33
26	Thermal properties of U–Mo alloys irradiated to moderate burnup and power. Journal of Nuclear Materials, 2015, 464, 331-341.	1.3	33
27	Electron energy-loss spectroscopy of anomalous plutonium behavior in nuclear waste materials. Micron, 2004, 35, 235-243.	1.1	31
28	Uranium*. , 2010, , 253-698.		30
29	Physical and Chemical Characterization of Actinides in Soil from Johnston Atoll. Environmental Science & Technology, 1997, 31, 467-471.	4.6	27
30	Precipitation of Nitrateâ^'Cancrinite in Hanford Tank Sludge. Environmental Science & Technology, 2004, 38, 4432-4438.	4.6	27
31	Time-Resolved Infrared Reflectance Studies of the Dehydration-Induced Transformation of Uranyl Nitrate Hexahydrate to the Trihydrate Form. Journal of Physical Chemistry A, 2015, 119, 9996-10006.	1.1	27
32	Detecting low levels of transuranics with electron energy loss spectroscopy. Ultramicroscopy, 1997, 67, 69-75.	0.8	26
33	10. Uranium Mineralogy and the Geologic Disposal of Spent Nuclear Fuel. , 1999, , 475-498.		25
34	Nanostructure of metallic particles in light water reactor used nuclear fuel. Journal of Nuclear Materials, 2015, 461, 236-243.	1.3	25
34	Nanostructure of metallic particles in light water reactor used nuclear fuel. Journal of Nuclear Materials, 2015, 461, 236-243. Getters for improved technetium containment in cementitious waste forms. Journal of Hazardous Materials, 2018, 341, 238-247.	1.3 6.5	25 25

#	Article	IF	CITATIONS
37	Long-Term Comparison of Dissolution Behavior Between Fully Radioactive and Simulated Nuclear Waste Glasses. Nuclear Technology, 1993, 104, 193-206.	0.7	23
38	Biotic and Abiotic Reduction and Solubilization of Pu(Ⅳ)O2•xH2O(am) as Affected by Anthraquinone-2,6-disulfonate (AQDS) and Ethylenediaminetetraacetate (EDTA). Environmental Science & Technology, 2012, 46, 2132-2140.	4.6	20
39	Revisiting the Growth Mechanism of Hierarchical Semiconductor Nanostructures: The Role of Secondary Nucleation in Branch Formation. Journal of Physical Chemistry Letters, 2019, 10, 6827-6834.	2.1	20
40	Incorporation of cerium and neodymium in uranyl phases. Journal of Nuclear Materials, 2006, 353, 147-157.	1.3	17
41	Nanoscale oxygen defect gradients in UO2+x surfaces. Proceedings of the National Academy of Sciences of the United States of America, 2019, 116, 17181-17186.	3.3	17
42	Characterization of High Phosphate Radioactive Tank Waste and Simulant Development. Environmental Science & Technology, 2009, 43, 7843-7848.	4.6	15
43	Synthesis and preservation of graphene-supported uranium dioxide nanocrystals. Journal of Nuclear Materials, 2016, 475, 113-122.	1.3	15
44	Can Cr(<scp>iii</scp>) substitute for Al(<scp>iii</scp>) in the structure of boehmite?. RSC Advances, 2016, 6, 107628-107637.	1.7	15
45	Focused ion beam for improved spatially-resolved mass spectrometry and analysis of radioactive materials for uranium isotopic analysis. Talanta, 2020, 211, 120720.	2.9	15
46	Neutron irradiation induced changes in isotopic abundance of 6Li and 3D nanoscale distribution of tritium in LiAlO2 pellets analyzed by atom probe tomography. Materials Characterization, 2021, 176, 111095.	1.9	15
47	The geochemical behaviour of Tc, Np and Pu in spent nuclear fuel in an oxidizing environment. Geological Society Special Publication, 2004, 236, 65-88.	0.8	14
48	Chemical stabilization of Hanford tank residual waste. Journal of Nuclear Materials, 2014, 446, 246-256.	1.3	14
49	Characterization of fission gas bubbles in irradiated U-10Mo fuel. Materials Characterization, 2017, 131, 459-471.	1.9	14
50	Nature of nano-sized plutonium particles in soils at the Hanford Site. Radiochimica Acta, 2014, 102, 1059-1068.	0.5	13
51	Sequestration of radioactive iodine in silver-palladium phases in commercial spent nuclear fuel. Journal of Nuclear Materials, 2016, 482, 229-235.	1.3	13
52	Uranium-contaminated soils: Ultramicrotomy and electron beam analysis. Microscopy Research and Technique, 1995, 31, 174-181.	1.2	11
53	Grain Boundary Corrosion and Alteration Phase Formation During the Oxidative Dissolution of UO2 Pellets. Materials Research Society Symposia Proceedings, 1996, 465, 519.	0.1	11
54	Fission recoil-induced microstructural evolution of the fuel-cladding interface [FCI] in high burnup BWR fuel. Journal of Nuclear Materials, 2019, 521, 120-125.	1.3	11

#	Article	IF	CITATIONS
55	Distribution of metallic fission-product particles in the cladding liner of spent nuclear fuel. Npj Materials Degradation, 2020, 4, .	2.6	11
56	Effects of electron irradiation of barium titanate. Radiation Effects and Defects in Solids, 1995, 133, 15-25.	0.4	10
57	Verifying the presence of low levels of neptunium in a uranium matrix with electron energy-loss spectroscopy. Micron, 2010, 41, 65-70.	1.1	10
58	Single-pass flow-through test elucidation of weathering behavior and evaluation of contaminant release models for Hanford tank residual radioactive waste. Applied Geochemistry, 2013, 28, 119-127.	1.4	10
59	<i>In situ</i> microscopy across scales for the characterization of crystal growth mechanisms: the case of europium oxalate. CrystEngComm, 2018, 20, 2822-2833.	1.3	10
60	Formation of Technetium Salts in Hanford Lowâ€Activity Waste Glass. Journal of the American Ceramic Society, 2016, 99, 3924-3931.	1.9	9
61	Identification of Uranyl Minerals Using Oxygen Kâ€Edge Xâ€Ray Absorption Spectroscopy. Geostandards and Geoanalytical Research, 2016, 40, 135-148.	1.7	9
62	Monitoring bromide effect on radiolytic yields using <i>in situ</i> observations of uranyl oxide precipitation in the electron microscope. RSC Advances, 2018, 8, 18227-18233.	1.7	9
63	Chemical and Isotopic Characterization of Noble Metal Phase from Commercial UO ₂ Fuel. Analytical Chemistry, 2019, 91, 6522-6529.	3.2	9
64	Development and Validation of Capabilities to Measure Thermal Properties of Layered Monolithic U–Mo Alloy Plate-Type Fuel. International Journal of Thermophysics, 2014, 35, 1476-1500.	1.0	8
65	Spontaneous redox continuum reveals sequestered technetium clusters and retarded mineral transformation of iron. Communications Chemistry, 2020, 3, .	2.0	8
66	An Atomic-Scale Understanding of UO ₂ Surface Evolution during Anoxic Dissolution. ACS Applied Materials & Interfaces, 2020, 12, 39781-39786.	4.0	8
67	Interfacial Engineering with a Nanoparticle-Decorated Porous Carbon Structure on β″-Alumina Solid-State Electrolytes for Molten Sodium Batteries. ACS Applied Materials & Interfaces, 2022, 14, 25534-25544.	4.0	8
68	Spectroscopic characterization of actinide materials. MRS Bulletin, 2010, 35, 889-895.	1.7	7
69	Controls on Soluble Pu Concentrations in PuO ₂ /Magnetite Suspensions. Environmental Science & Technology, 2012, 46, 11610-11617.	4.6	7
70	Stamping Nanoparticles onto the Electrode for Rapid Electrochemical Analysis in Microfluidics. Micromachines, 2021, 12, 60.	1.4	7
71	Waste Glass Weathering. Materials Research Society Symposia Proceedings, 1993, 333, 41.	0.1	6
72	Observation of aqueous Cm(III)/Eu(III) and UO22+ nanoparticulates at concentrations approaching solubility limit by laser-induced fluorescence spectroscopy. Journal of Alloys and Compounds, 2006, 418, 166-170.	2.8	6

#	Article	IF	CITATIONS
73	Thermal properties of U-Mo alloys irradiated under high fission power density. Journal of Nuclear Materials, 2021, 547, 152823.	1.3	6
74	A Review of Bismuth(III)-Based Materials for Remediation of Contaminated Sites. ACS Earth and Space Chemistry, 2022, 6, 883-908.	1.2	6
75	Formation and growth of cerium (III) oxalate nanocrystals by liquid-cell transmission electron microscopy. Scripta Materialia, 2022, 219, 114856.	2.6	5
76	Solution-Borne Colloids from Drip Tests using actinide-Doped and Fully-Radioactive Waste Glasses. Materials Research Society Symposia Proceedings, 1996, 465, 165.	0.1	4
77	Sensitivity of UO2 Stability in a Reducing Environment on Radiolysis Model Parameters. Materials Research Society Symposia Proceedings, 2012, 1444, 3.	0.1	4
78	Conditions for Critical Effects in the Mass Action Kinetics Equations for Water Radiolysis. Journal of Physical Chemistry A, 2014, 118, 12105-12110.	1.1	4
79	In situ liquid SIMS analysis of uranium oxide. Surface and Interface Analysis, 2020, 52, 454-459.	0.8	4
80	Neptunium Incorporation into Uranium(Vi) Compounds formed During Aqueous Corrosion of Neptunium-Bearing Uranium Oxides. Materials Research Society Symposia Proceedings, 2002, 713, 1.	0.1	3
81	Evidence for Neptunium Incorporation into Uranium (VI) Phases. Materials Research Society Symposia Proceedings, 2004, 824, 538.	0.1	3
82	Radiolytic microscale power generation based on single chamber fuel cell operation. Journal of Micromechanics and Microengineering, 2007, 17, S250-S256.	1.5	3
83	Spectroscopic studies of the several isomers of UO3. , 2013, , .		3
84	Heterogeneous reduction of 239PuO2 by aqueous Fe(II) in the presence of hematite. Radiochimica Acta, 2013, 101, 701-710.	0.5	3
85	Dehydration of uranyl nitrate hexahydrate to uranyl nitrate trihydrate under ambient conditions as observed via dynamic infrared reflectance spectroscopy. Proceedings of SPIE, 2015, , .	0.8	3
86	Effects of hydrated lime on radionuclides stabilization of Hanford tank residual waste. Chemosphere, 2017, 185, 171-177.	4.2	3
87	Determination of the degree of grain refinement in irradiated U-Mo fuels. Heliyon, 2018, 4, e00920.	1.4	3
88	Unveiling the Early Stages of the F-element Oxalate Growth Evolution with Cryo-TEM. Microscopy and Microanalysis, 2020, 26, 642-644.	0.2	3
89	A new non-diffusional gas bubble production route in used nuclear fuel: implications for fission gas release, cladding corrosion, and next generation fuel design. Physical Chemistry Chemical Physics, 2020, 22, 6086-6099.	1.3	3
90	Studying Corrosion Using Miniaturized Particle Attached Working Electrodes and the Nafion Membrane. Micromachines, 2021, 12, 1414.	1.4	3

#	Article	IF	CITATIONS
91	Formation of Tc metal in 12ÂM HCl using Zn as a reductant. Journal of Radioanalytical and Nuclear Chemistry, 2013, 298, 1315-1321.	0.7	2
92	Performance evaluation and post-irradiation examination of a novel LWR fuel composed of U0.17ZrH1.6 fuel pellets bonded to Zircaloy-2 cladding by lead bismuth eutectic. Journal of Nuclear Materials, 2017, 486, 391-401.	1.3	2
93	A microfluidic electrochemical cell for studying the corrosion of uranium dioxide (UO ₂). RSC Advances, 2022, 12, 19350-19358.	1.7	2
94	Comment on â€~Extended electron energy loss fine structure simulation of the local boron environment in sodium aluminosilicate glasses containing gadolinium' by M. Qian, H. Li, L. Li and D.M. Strachan [J. Non-Cryst. Solids 328 (2003) 90]. Journal of Non-Crystalline Solids, 2005, 351, 184-185.	1.5	1
95	An electrochemical technique for controlled dissolution of zirconium based components of light water reactors. RSC Advances, 2019, 9, 1869-1881.	1.7	1
96	Formation of pyrophosphates across grain boundaries induces the formation of mismatched but oriented interfaces in silver phosphate polypods. Applied Surface Science, 2021, 563, 149980.	3.1	1
97	Investigation of the Oxidation State of Uranium in Nuclear Materials and their Alteration Products. Materials Research Society Symposia Proceedings, 2002, 713, 1.	0.1	0
98	Investigations into the polymorphs and hydration products of UO ₃ . , 2012, , .		0
99	Technetium Incorporation into C14 and C15 Laves Intermetallic Phases. Materials Research Society Symposia Proceedings, 2013, 1518, 117-122.	0.1	Ο
100	The solubility of 242PuO2 in the presence of aqueous Fe(II): the impact of precipitate preparation. Radiochimica Acta, 2014, 102, 861.	0.5	0
101	Correlative Microscopic, Spectroscopic, and Computational Analysis of the Nucleation and Growth of Europium (III) Oxalate Nanoparticles. Microscopy and Microanalysis, 2016, 22, 1396-1397.	0.2	0
102	Nanoscale Quantification of Interstitial Oxygen in Hyperstoichiometric UO2+x. Microscopy and Microanalysis, 2019, 25, 1598-1599.	0.2	0
103	In Operando SEM Imaging of Electrochemical Oxidation of UO2 in Liquid. Microscopy and Microanalysis, 2019, 25, 1578-1579.	0.2	0
104	Targeted uranium recovery from complex alloys using fluoride volatility. Journal of Fluorine Chemistry, 2020, 235, 109539.	0.9	0
105	Nanoscale Diffusion of Lead in 300Ma Old UTi2O6 Mineral. Microscopy and Microanalysis, 2020, 26, 172-174.	0.2	0
106	Studying the UO2 Electrochemistry In Situ Using SEM. Microscopy and Microanalysis, 2020, 26, 1790-1792.	0.2	0
107	Cryo-TEM Characterization of the Early Stages of the Uranium Oxalate Growth Evolution. Microscopy and Microanalysis, 2021, 27, 1940-1941.	0.2	0
108	Making electrodes by particle stamping for microscopic and electrochemical analysis. Microscopy and Microanalysis, 2021, 27, 2504-2506.	0.2	0

#	Article	IF	CITATIONS
109	Solubility controls on plutonium and americium release in subsurface environments exposed to acidic processing wastes. Applied Geochemistry, 2023, 153, 105241.	1.4	ο